

We are IntechOpen, the world's leading publisher of Open Access books Built by scientists, for scientists

6,900

Open access books available

186,000

International authors and editors

200M

Downloads

Our authors are among the

154

Countries delivered to

TOP 1%

most cited scientists

12.2%

Contributors from top 500 universities



WEB OF SCIENCE™

Selection of our books indexed in the Book Citation Index
in Web of Science™ Core Collection (BKCI)

Interested in publishing with us?
Contact book.department@intechopen.com

Numbers displayed above are based on latest data collected.
For more information visit www.intechopen.com



FEA and Experimentally Determination of Applied Elasticity Problem for Fabricating Aspheric Surfaces

Duc-Nam Nguyen

Abstract

The elastic deformation machining method is suitable for fabricating aspheric surfaces that have excellent physical properties of elastic materials. The machining process is carried out with the deformation model without mold. When vacuum pressure is supplied to the workpiece, the top surfaces of workpiece are deformed into aspheric shape. After machining process, the bottom surface will be formed into the aspheric shape and the top surface returns to its original flat surface form due to internal force and bending moments of the material. However, the accuracy will decrease due to the reduced thickness while the vacuum pressure keeps unchanged during machining process. Therefore, it is necessary to carry out the finite element analysis (FEA) to determine the vacuum pressure with corresponding to the reduced thickness. In addition, the mold with its surface approximates and the desired surface form of the lens is also presented. When uniform vacuum pressure is supplied to the workpiece through small holes of the mold, the workpiece will be deformed into aspheric profile as similar to the mold surfaces. In order to improving the form accuracy, the FEA and the experiment are studied for modifying the mold profile to correspond with bending strength of workpiece material.

Keywords: elastic deformation, aspheric surface, glass lapping, glass molding, vacuum pressure, experimental study, finite element analysis

1. Introduction

Nowadays, for managing laser light in sophisticated and compact laser systems, aspheric lenses are the most powerful lenses. In these systems, it is generally accepted that spherical aberration is the most common performance detractor. From the use of spherical surfaces, it is found that they artificially limit focusing and collimating accuracy. In spite of the fact that spherical geometry is not optimal for refracting light that has been known for centuries, the high cost and difficulty of fabricating nonspherical (aspheric) surfaces has inhibited them from a wider use.

Because aspheric surfaces offer advantages such as high resolution, light weight, and low cost, they are widely used in the opto-electronics industry. As aspheric surfaces are more effective in shaping the light than spherical surfaces, they have

recently been used in measurement instruments, astronomy, and optical lens [1, 2]. **Figure 1** shows some applications which employ aspheric surfaces.

In most general terms, an optical lens can be determined as a refracting device that reconfigures the light wave front incident upon it. The phase, direction of propagation, intensity, and polarization state are the properties of the incident light beam which are influenced by a lens. Surface form and roughness, diameter, sub-surface defects generated during the fabrication process, shape accuracy, physical and mechanical properties of the optical material, and other optical conditions, such as the angle of incidence of light beam, absorption, reflection, and environmental influences, are some of the major characteristics that govern the performance of an optical lens [3].

To overcome the aberration problems of spherical lenses, a number of spherical surfaces with different signs of aberrations have to be utilized to balance and minimize the final aberration to obtain high quality images. In principle, the optical system designer can always use enough spherical lenses to simultaneously correct for all of the common optical aberrations in a lens system if the number of elements used in an optical system is not limited. The number of surfaces required to do this may be so large that the resulting lens assembly is excessively large in size and weight, and expensive to produce. In addition, the transmission of the assembly lens may be unduly reduced due to the residual reflections from each surface, and the bulk absorption in each lens.

The usage of aspheric surfaces, both with and without the incorporation of diffractive elements, allows the design and construction of assembly lens with the same or even better optical performance than an equivalent all-spherical system. However, in most cases, with a significant reduction in the number of elements required, there is a significant improvement in the overall lens assembly size, weight, cost, and optical transmission. In many cases, in an optical system, each aspheric surface can be applied to replace at least two other spherical surfaces. Hence, aspheric lenses are more efficient because additional error-correcting lenses are not required. **Figure 2** is an illustration of spherical and aspheric lens systems.

Cutting techniques such as turning and milling processes are usually utilized for the production of aspheric glass lenses as shown in **Figure 3**.

The machining processes, which usually consist of computer numerically controlled (CNC) generators, are employed to machine an aspheric shape on a lens to generate the desired shape. In glass machining, the roughness on a cutting edge has a larger effect on surface finish than that of metal machining. Glass workpiece can be machined without brittle fractures with an undeformed chip thickness less than $1\ \mu\text{m}$ in milling and turning processes [4–7].

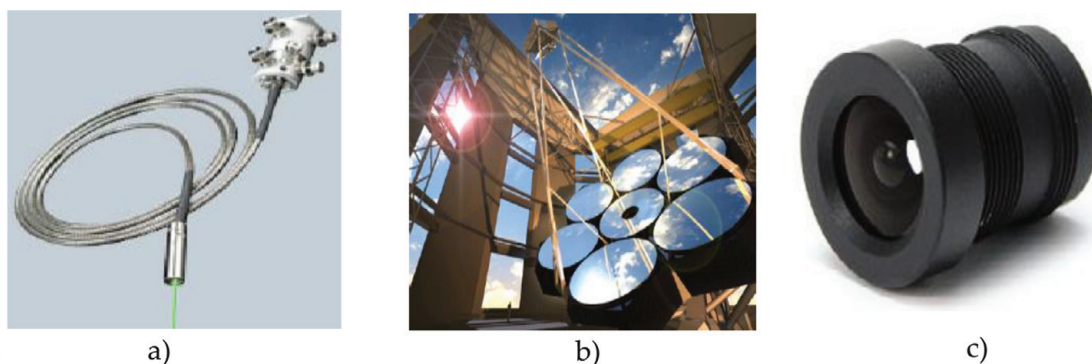


Figure 1. Application of aspheric surfaces: (a) measurement instruments, (b) astronomy, and (c) optical lens.

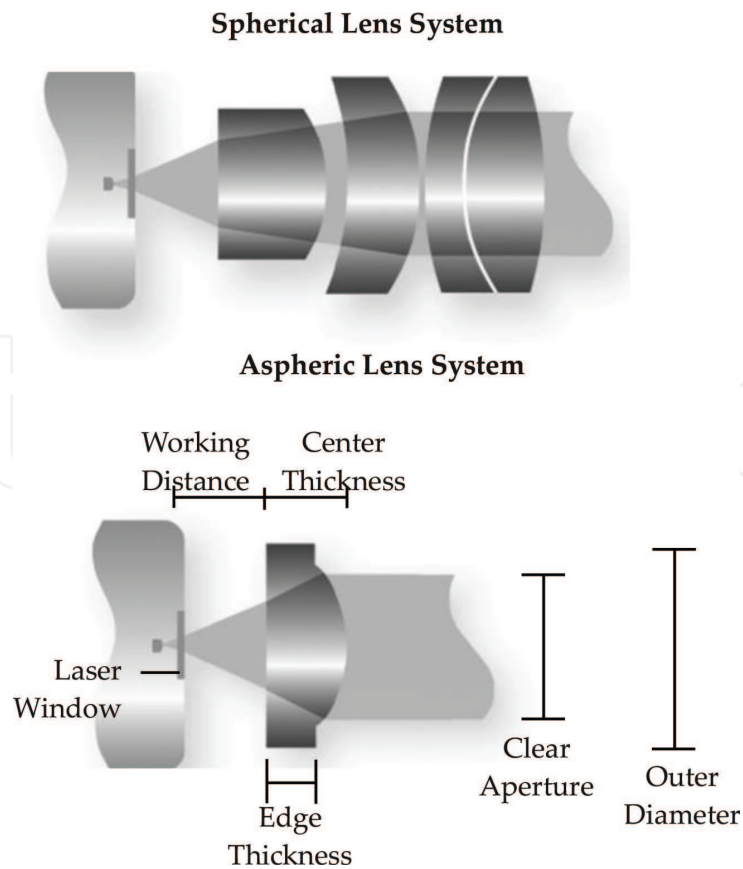


Figure 2.
Spherical vs. aspheric lens systems.

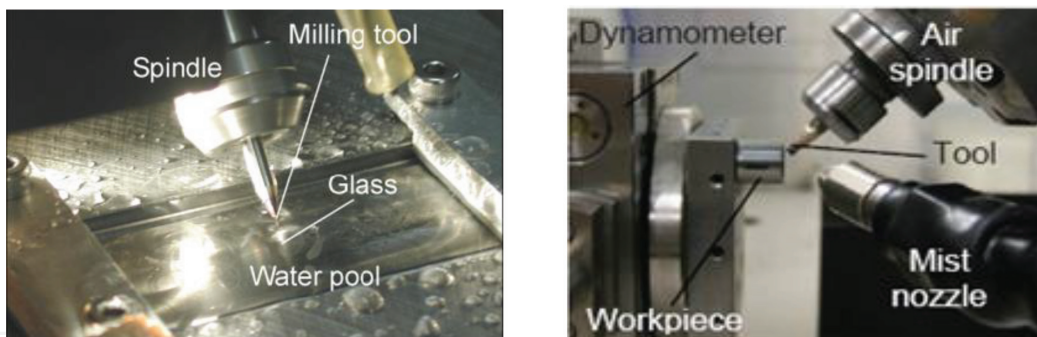


Figure 3.
Schematic illustration of milling and turning processes.

Thereafter, the optical lenses are fine machined by grinding, and then followed by polishing to achieve the good surfaces. In the grinding process, if the depth of cut is below a certain value, the material removal mode is ductile flow which is characterized by low surface roughness and subsurface damage [8–12]. **Figure 4** is an illustration of a precision grinding process.

“Precessions” polishing is an automated polishing method that uses a 7-axis CNC machine tool for polishing spherical and aspheric surfaces [13, 14]. Based on contact between the workpiece surface and polishing tool, the polishing spot of desired size is generated by controlling the load cell in polishing process. The polishing tool then moves in angular steps around the local normal to the part surface during machining process. The 7-axis CNC capability of the machine also makes the generation of free-form surfaces possible. **Figure 5** shows a schematic illustration of a “Precessions” polishing process.

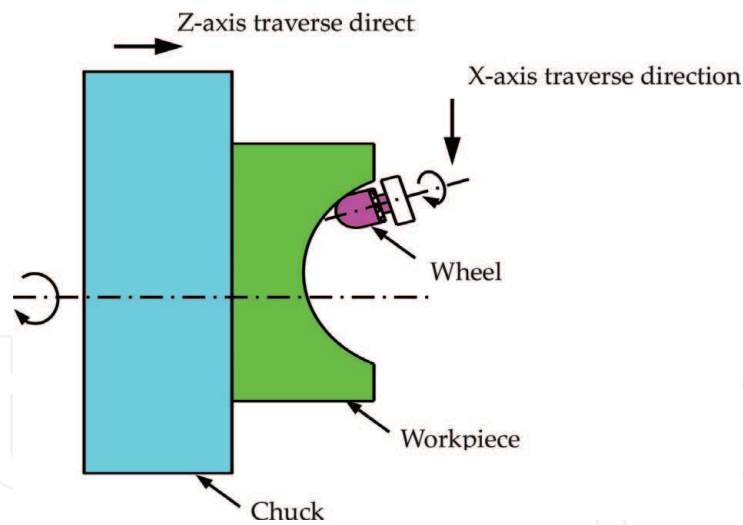


Figure 4.
Schematic illustration of a precision grinding process.

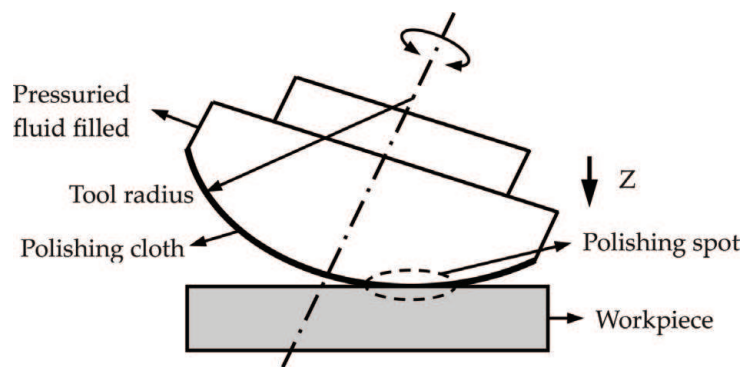


Figure 5.
Schematic illustration of a "Precessions" polishing process.

To fabricate aspheric surfaces, the movement of the tool must be constrained in the machining process. A sub-aperture tool (smaller in size than the lens) on a modified polishing machine is then utilized, and by controlling the amount of time the tool spends working at a given lens location, a desired aspheric surface can be fabricated. In addition to the complexity of the machining processes, conventional aspheric fabrication is highly sensitive to the manufacturing conditions, which strongly depend on the positioning accuracy of the machine, the condition of the grinding wheel, and the vibrations in the system. These factors result in an expensive manufacturing cost and a low production yield.

Compared to traditional cold-working methods, glass molding and precision injection molding have greatly advanced the fabrication technologies for aspheric lens industry because of their unique advantages such as excellent compatibility, high efficiency, great flexibility, and high consistency [15–17]. The mass production of aspheric glass lenses is fabricated by applying the technologies. In the glass molding technique, a glass lens is fabricated by compressing glass melting at a high temperature and replicating the shapes of the mold without any need of further machining. **Figure 6a** shows the process begins by putting a glass gob on top of a lower mold. Both the glass gob and the mold are heated to a molding temperature above the transition temperature of glass (**Figure 6b**). After the glass and the mold temperature have reached a steady state molding temperature, the mold is closed by moving the lower mold (**Figure 6c**). The temperature is maintained during the molding step. All steps are performed in vacuum environment. Then, by holding

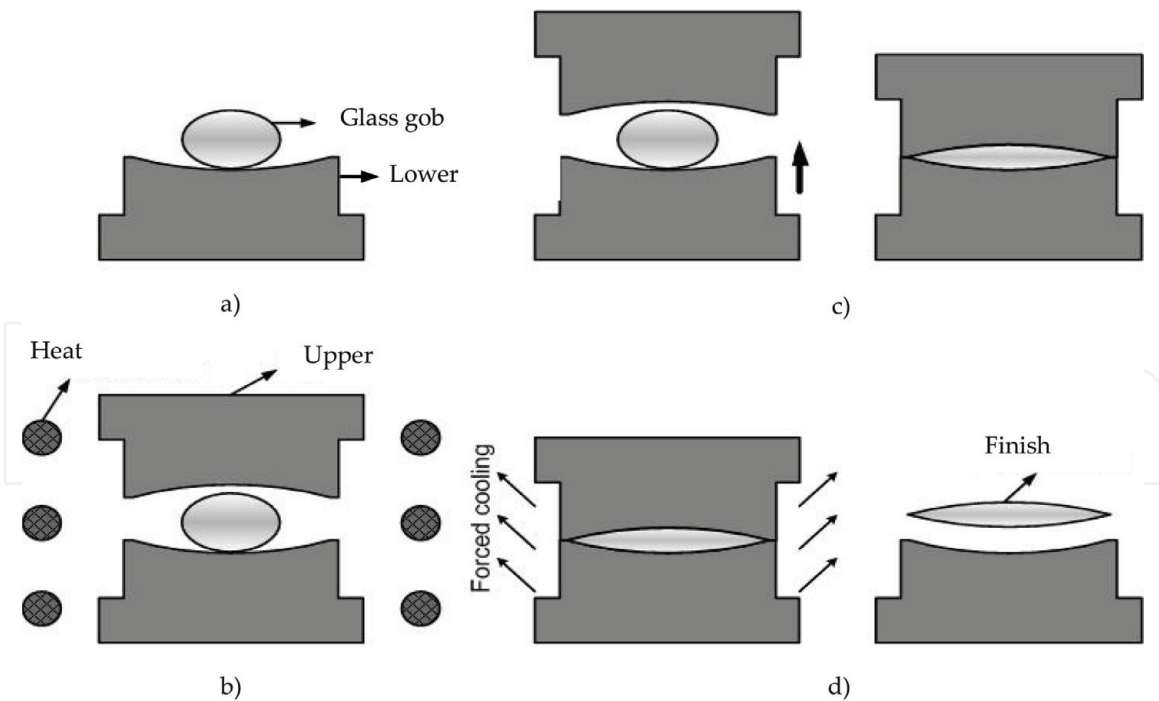


Figure 6. Schematic illustration of a lens molding process: (a) Molds and glass gob, (b) Heating, (c) Heating and pressing, and (d) Cooling and release.

the pressed load for a short time at a slow cooling rate, the stress in the glass lens is relaxed. Lastly, the formed glass lens is rapidly cooled to ambient temperature and released from the molds (**Figure 6d**). A BK7 glass fabricated using this molding process has surface roughness of approximately 5 nm Ra , and form accuracy of 0.2 μm $P-V$.

In spite of the obvious advantages, there are serious drawbacks that currently limit the application of injection molding and glass molding technologies to smaller size aspheric lens fabrications. A typical drawback is the altering of optical properties such as refractive index, due to heating and annealing of the glass material, and the uneven shrinking due to the cooling process that causes error in lens profile [18].

In contrast, the elastic deformation machining method is a good technique that the workpiece will be deformed into aspheric shape prior to the lapping process under vacuum pressure. While the vacuum pressure is remained, the opposite side is polished to optical flatness by the lapping wheel. When the vacuum pressure is released, the bottom surface of the workpiece will be shaped into an aspheric shape and the top surface will restore to its flat surface form by internal force and bending moments. Consequently, for machining materials which have excellent physical properties due to their perfect crystal structures, the elastic deformation method is appropriate [19].

2. Theory of elastic deformation

Based on the elasticity of the material, the circular flat plate is deformed to an aspheric surface by applying the pressure in the elastic deformation machining method. The deflection of the circular plate can be calculated by using appropriate plate theory. There are two types of edge support for circular plate, such as fixed (or clamped) edge and simply supported edge which are considered in this section.

2.1 Basic equations for circular plate in elastic deformation

The amount of deflection of circular plate can be determined by solving the differential equations of an appropriate plate theory [20]. Two types of edge support include clamped and simply supported edge which are used in the elastic deformation method. In the case of simple bending of circular plate, the amount of deflection w is assumed to be very small in comparison with plate thickness. According to the small deflection theory of thin homogenous elastic plates, the deformation in the middle plane of the plate can be neglected and the straight line initially normal to the middle surface to the plate remains straight. In addition, the stress (i.e., transverse normal stress) is small when compared to other stress components and should be neglected in stress-strain relationship. Under these conditions, the three dimensional plate problem can be reduced to two dimensions. The linear theory of elasticity can be used to derive the governing differential equation for a plate subject to uniform transverse loads. The equation for small deformation w of a thin circular plate of constant thickness h is:

$$D \cdot \nabla^2(\nabla^2 w) - p = 0; D = Eh^3/12(1 - \nu^2) \quad (1)$$

E and ν are the Young's modulus and Poisson's coefficient. D is the rigidity constant of the plate, and p is the load on the plate. Because of the rotational symmetry, the Laplacian operator ∇^2 in polar coordinates r and θ can be written as:

$$\nabla^4 w = \left(\frac{\partial^2}{\partial r^2} + \frac{1}{r} \frac{\partial}{\partial r} + \frac{1}{r^2} \frac{\partial^2}{\partial \theta^2} \right) \left(\frac{\partial^2 w}{\partial r^2} + \frac{1}{r} \frac{\partial w}{\partial r} + \frac{1}{r^2} \frac{\partial^2 w}{\partial \theta^2} \right) \quad (2)$$

The moment can be written in the form,

$$M_r = -D \left[\frac{\partial^2 w}{\partial r^2} + \nu \left(\frac{1}{r^2} \frac{\partial^2 w}{\partial \theta^2} + \frac{1}{r} \frac{\partial w}{\partial r} \right) \right] \quad (3)$$

$$M_t = -D \left[\frac{1}{r} \frac{\partial w}{\partial r} + \frac{1}{r^2} \frac{\partial^2 w}{\partial \theta^2} + \nu \frac{\partial^2 w}{\partial r^2} \right] \quad (4)$$

where M_r and M_t are radial moment and tangential moment.

If the load acting on the plate is symmetrically distributed about the axis perpendicular to the middle plane of the plate, the deflection w is independent of θ , when Eqs. (3) and (4) becomes:

$$\left(\frac{d}{dr^2} + \frac{1}{r} \frac{d}{dr} \right) \left(\frac{d^2 w}{dr^2} + \frac{1}{r} \frac{dw}{dr} \right) = \frac{p}{D} \quad (5)$$

In other form, it shown as

$$\left(\frac{d^2 w}{dr^2} + \frac{1}{r} \frac{dw}{dr} \right) = \frac{1}{r} \frac{d}{dr} \left(r \frac{dw}{dr} \right) \quad (6)$$

Eq. (5) can be written as

$$\frac{1}{r} \frac{d}{dr} \left\{ r \frac{d}{dr} \left[\frac{1}{r} \frac{d}{dr} \left(r \frac{dw}{dr} \right) \right] \right\} = \frac{p}{D} \quad (7)$$

Multiply both sides of Eq. (6) by r and then integrate to obtain,

$$r \frac{d}{dr} \left[\frac{1}{r} \frac{d}{dr} \left(r \frac{dw}{dr} \right) \right] = \frac{pr^2}{2D} + C_1 \quad (8)$$

or,

$$\frac{d}{dr} \left[\frac{1}{r} \frac{d}{dr} \left(r \frac{dw}{dr} \right) \right] = \frac{pr}{2D} + \frac{C_1}{r} \quad (9)$$

By successive integrations, the deflection can arrive finally at

$$w_r = \frac{pr^4}{64D} + C_1 r^2 \ln r + C_2 r^2 + C_3 \ln r + C_4 \quad (10)$$

The shears for the symmetrically loaded plate can be given as follow,

$$\frac{d}{dr} \left(\frac{d^2 w}{dr^2} + \frac{1}{r} \frac{dw}{dr} \right) = -\frac{Q}{D} \quad (11)$$

and from Eq. (9),

$$\frac{pr}{2D} + \frac{C_1}{r} = -\frac{Q}{D} \quad (12)$$

This equation indicates that Q would approach infinity as r approaches zero. To prevent this from happening, we make $C_1 = 0$. From Eq. (10), it can be seen that w becomes infinity at $r = 0$. To avoid this, the constant C_3 must be zero. Thus,

$$w_r = \frac{pr^4}{64D} + C_2 r^2 + C_4 \quad (13)$$

From Eq. (13), the amount of deflection w_r is the function of r in cylindrical coordinate system.

2.2 Circular plate with simply supported edge

The boundary conditions are $w = 0$ and $M_r = 0$ at $r = a$.

Eq. (13) can be written,

$$\frac{pa^4}{64D} + C_2 a^2 + C_4 = 0 \quad (14)$$

and

$$\frac{pa^2}{64} (12 + 4\nu) + \frac{C_2}{2} (1 + \nu) = 0 \quad (15)$$

From the equations, we can find

$$C_2 = -\frac{pa^2}{32D} \frac{3 + \nu}{1 + \nu}; C_4 = \frac{pa^4}{64D} \frac{5 + \nu}{1 + \nu} \quad (16)$$

so that the deflection of every radial location can be calculated using,

$$w_r = \frac{p(a^2 - r^2)}{64D} \left[\frac{5 + \nu}{1 + \nu} a^2 - r^2 \right] \quad (17)$$

The maximum deflection which occurs at $r = 0$, is given by,

$$w_0 = \frac{pa^4}{64D} \left(\frac{5 + \nu}{1 + \nu} \right) \quad (18)$$

Substitute $D = Eh^3/12(1 - \nu^2)$ into Eq. (18), we have:

$$w_0 = \frac{3p(1 - \nu)(5 + \nu)a}{16E} \left(\frac{a}{h} \right)^3 \quad (19)$$

From Eq. (19), we can see that the maximum deflection of the circular plate is relative of the diameter a and the ratio between diameter a and thickness h .

3. Elastic deformation machining method without mold

Figure 7 shows a schematic illustration of a lens elastic deformation process without mold.

Two surfaces of the workpiece are polished to certain flatness before fabricating as shown in **Figure 7a**. When vacuum pressure is supplied to the workpiece through

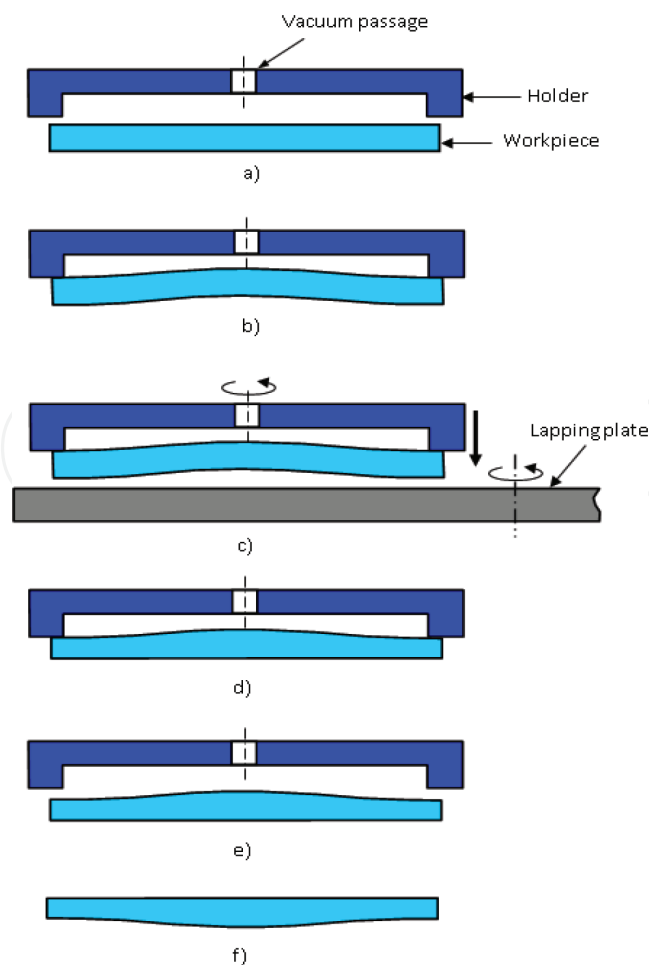


Figure 7.
(a-f) Schematic illustration of an aspheric surface elastic deformation process.

a hole, the workpiece is deformed in the middle. The edge of the workpiece is supported by the holder; therefore, it will be not moved. This makes the workpiece become a formed aspheric shape as presented in **Figure 7b**. The deflection of the workpiece can be calculated by using theoretical equation in boundary conditions of circular plate with simply supported edge. While the vacuum pressure is still remained, the workpiece and the holder start rotating and moving downward in contact with the lapping plate. Its opposite side will be polished to optical flatness as illustrated in **Figure 7c** and **d**. Then, the vacuum pressure is not supplied and the workpiece is also released from the holder as shown in **Figure 7e**. According to the **Figure 7f**, the bottom surface will be formed into the aspheric shape and the top surface returns to its original flat surface form due to material elasticity. It can be seen that the deformed workpiece surfaces can be restored by internal force and bending moments which are created from the vacuum pressure during machining process.

3.1 Finite element analysis for elastic deformation machining process

The vacuum pressure affects an amount of elastic deformation of the workpiece; hence, the accuracy of manufactured profile will also be highly dependent on the vacuum pressure as well. **Figure 8a** and **b** illustrates that the workpiece is lapped and polished to a flat surface while the vacuum pressure stays it at the initial deformed state.

The manufactured workpiece accuracy can be improved by adjusting the vacuum pressure during the machining process because of the changed workpiece thickness [21]. The vacuum pressure is defined by finite element analysis (FEA) results because theoretical calculation for complex surface is more difficult. In simulation process, a circular plate B270 optical glass with the edge supported by the holding device is listed in **Table 1**.

All elements of modeling were created by meshing with A20-node quadratic brick elements in reduced integration (C3D20R). **Figure 9** demonstrates the finite element model as follows.

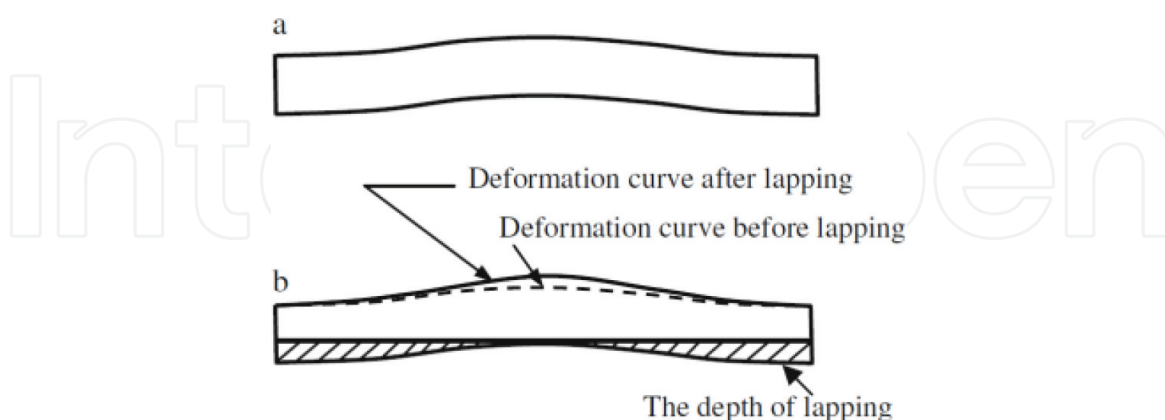


Figure 8. (a and b) The deforming and lapping processes of glass plate. (a) The glass plate is deformed before lapping and (b) the glass plate is deformed in lapping.

Density (kg/m ³)	Young's modulus (GPa)	Knoop hardness HK100 (kg/mm ²)	Poisson ratio
2550	71.5	542	0.22

Table 1. Material properties of B270 optical glass [22].

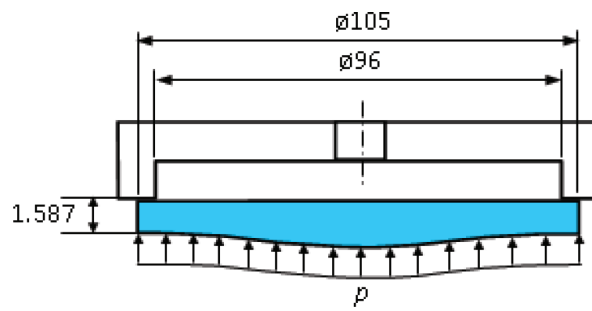


Figure 9.
Simulation model of workpiece.

When the vacuum pressure keeps unchanged, the workpiece thickness is reduced during the lapping process. Therefore, the surface form of a glass plate will have some errors compared to desired surface form at the end of the machining process. The results of the FEA indicate that the deflection of workpiece is greater than desired curve. In order to enhance its accuracy, the vacuum pressure should be fixed at 42 kPa as shown in **Figure 10**.

3.2 Experimental setup

The B270 optical glass which is a clear, high transmission and high purity raw materials is chosen in this experiment. The workpiece sides are lapped and polished to flat surfaces. The lapping process is through the relative motion between the lapping plate and the workpiece, affected by abrasive slurry under distribution load. The silicon carbide (SiC) and cerium oxide (CeO_2) abrasive grain slurry are used in the experiment. The principle of lapping process can be seen in **Figure 11**.

In lapping process, a rigid iron surface covered by a flannelette plate is moved under the load on the glass surface, with abrasive particles suspended in water between them. **Table 2** demonstrates parameters for the machining process. To remove microcrack layer and trace after the lapping process, a polishing step is required. This step is also carried out with the Nanopoli-100 precision polishing machine. The polishing parameters fixed unchanged as that in the initial lapping step, except that the abrasive is changed from SiC to CeO_2 as a fine polishing step.

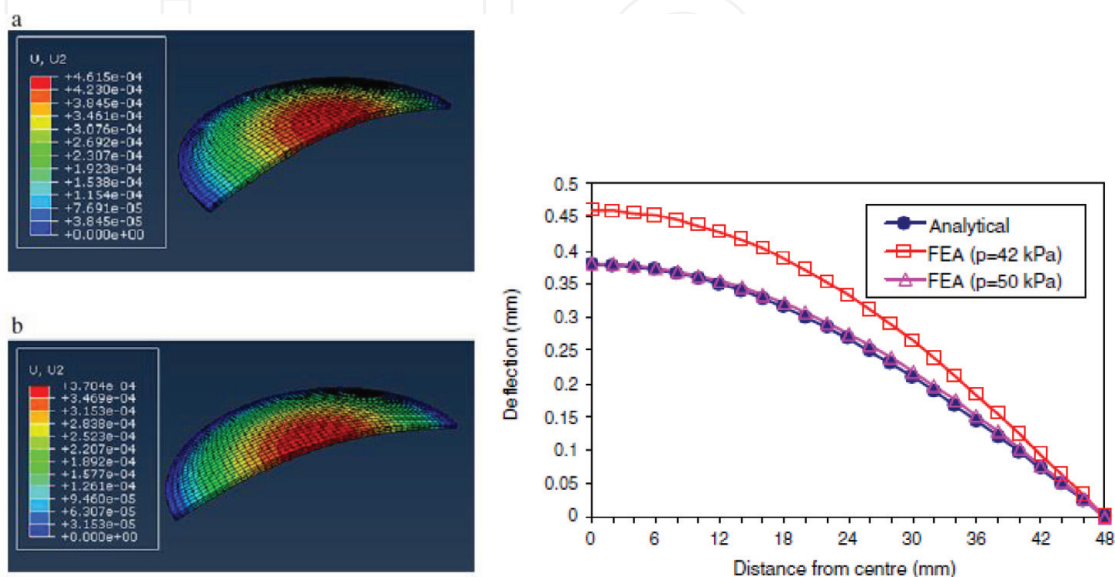


Figure 10.
Finite element analysis results and analytical results: (a) $P = 50 \text{ kPa}$ and (b) $P = 42 \text{ kPa}$.

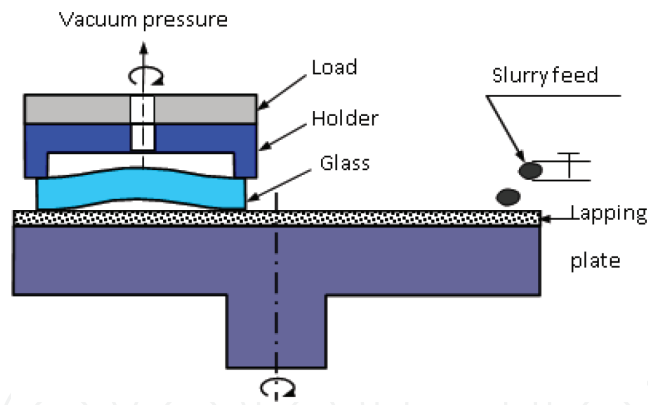


Figure 11.
 Principle of lapping and polishing process.

Items	Lapping	Polishing
Abrasive	#1000 SiC	#10,000 CeO ₂
Abrasive concentration in slurry (wt%)	10%	10%
Machining load (N)	20	15
Rotating speed of lapping plate (rpm)	60	40
Machining time (min)	240	60

Table 2.
 Lapping and polishing conditions.

3.3 Experimental results

The component accuracy can be improved by adjusting the vacuum pressure values to compensate for its lost thickness during the lapping step. The vacuum pressure is defined through FEA results. **Figure 10** shows that the deformation curve of the workpiece is close to the desired curve when the vacuum pressure is fixed at 42 kPa. Therefore, the vacuum pressure should be reduced from 50 to 42 kPa in the experiment. **Figure 12** illustrates the deflection and deviation results of the experimental results and the theoretical calculations.

Depending on reducing pressure from 50 to 42 kPa and keeping stable through the entire lapping step, the experimental results agree greatly with theoretical calculations. The peak-valley value is reached at 1.6 μm .

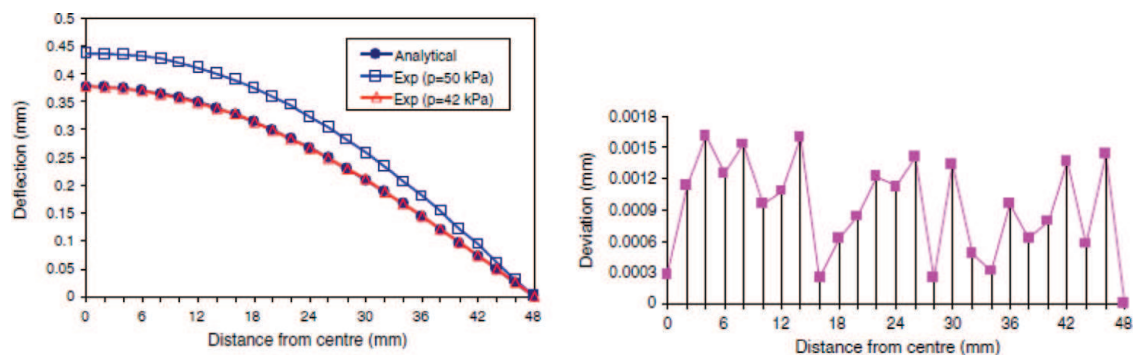


Figure 12.
 The experimental results of deflection and deviation against theoretical results.

4. Elastic deformation machining method with mold

In the elastic deformation machining process without mold, the thickness of the plate is reduced while the vacuum pressure remains unchanged. Thus, the workpiece deformation to increase as lapping progresses. This will cause large deviation in surface form between finished workpiece and theoretical calculation. The mold with its surface approximates the desired surface form of the lens which is used for improving the machining precision. When vacuum pressure is supplied, the top surface of the workpiece will be deformed and then contacts the molded surface. **Figure 13** shows the basic concept of elastic deformation molding process [23].

The mold and workpiece surfaces are polished to flatness before fabricating as shown in **Figure 13a**. When uniform vacuum pressure is supplied to the workpiece through small holes of the mold, the workpiece will be deformed and then contacted with the aspheric surface of the mold as presented in **Figure 13b**. While deformed workpiece is kept stable under vacuum pressure, the bottom side of the workpiece is polished to flatness as illustrated in **Figure 13c** and **d**. Then, the vacuum pressure is not supplied; hence, the lapped side of workpiece will be formed into the mold surface while the opposite surface returns to its original flatness surface due to material elasticity as shown in **Figure 13e**.

4.1 Finite element analysis for elastic deformation machining process with mold

The standard aspheric formula is:

$$Z = \frac{cr^2}{1 + \sqrt{1 - (1+k)c^2r^2}} + \sum_{i=2}^n A_{2i}r^{2i} \quad (20)$$

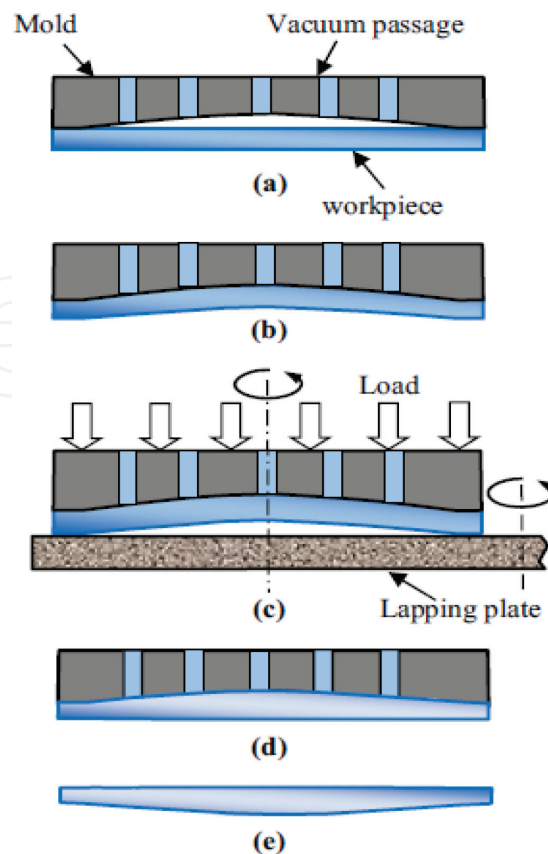


Figure 13.
Basic principle of elastic deformation molding process.

where Z , depth or “Sag” of the curve; r , distance from the center; c , curvature ($=1/\text{radius}$); K , conic constant; and A_{2i} , higher order terms.

The radius (R) is used for determining the aspheric terms such as their shallow or depth. The closest spherical surface is the radius which reaches the aspheric sag at the largest useful diameter [24]. **Figure 14** illustrates the aspheric lens sag.

An aspherical surface is built by using spherical surface combined with the higher order terms. Most optical designers use only the even-order terms from A_2 to A_{20} . The conic constant K has been used to design the initial aspheric, simple paraboloid and hyperboloid (as shown in **Table 3**).

In elastic deformation machining method, the accuracy of aspheric lens depends on the ability of elastic deformation and completely contacting the mold surfaces. The mold surface is defined by choosing the closest spherical surface (as shown in **Figure 15**). The FEA is designed for establishing the spherical surface through a simulation of contacting process between workpiece and mold surface.

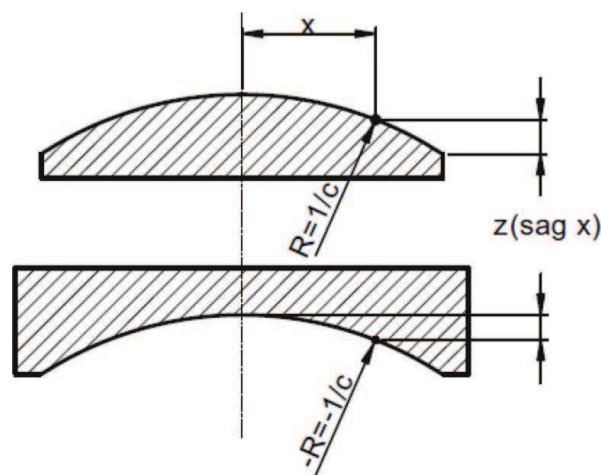


Figure 14.
 The sag of aspheric lens.

Conic constant	Surface type
$K = 0$	Spherical
$K = -1$	Paraboloid
$K < -1$	Hyperboloid
$-1 < K < 0$	Ellipsoid
$K > 0$	Oblate ellipsoid

Table 3.
 The relationship between conic constants and surface types.

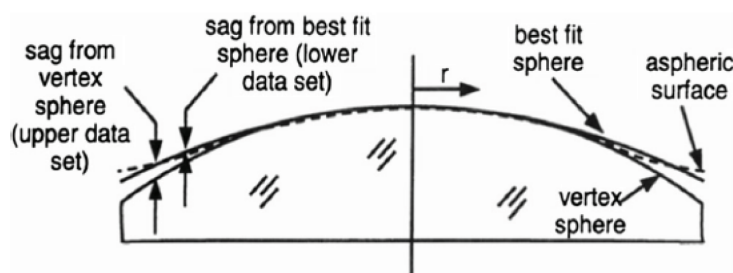


Figure 15.
 The aspheric surface from best fit sphere.

In the simulation process, the thickness ($h = 1.0$ mm) and diameter ($D = 50$ mm) of the workpiece are suggested. In addition, the radius ($R = 2500$ mm) of spherical surface is chosen. The parameters of FEA model can be seen in **Figure 16a**.

The axisymmetric model is selected in this simulation process. The mold is chosen as an analytical rigid shell and the workpiece is a deformable shell. The analytical step of model is “Dynamic, Explicit”. The interaction and the contact property are “Surface to surface contact” and “Penalty contact method,” respectively. All elements of the workpiece are divided in meshing with A4-node bilinear axisymmetric quadrilateral elements in reduced integration. The workpiece mesh and boundary conditions are described in **Figure 16b**. The values of uniform vacuum pressure are opted in range of -80 to -100 kPa. The conic constant $K = 0.25$ is selected for the simulation process.

It is clear to see that **Figure 17** shows the deflection and deviation of workpiece under different vacuum pressures with the conic constant $K = -3$.

According to the results, the model with the conic constant $K = -3$, gives the best one and the deviation between the workpiece and the mold is the smallest. The workpiece and the mold can reach the best when the vacuum pressure approximates -95 kPa. However, when the vacuum pressure is larger than -95 kPa, the deviation results are still stable. Therefore, the conic constant $K = -3$ recommends for defining the aspheric surface of the mold.

The accuracy one can be innovated by modifying the mold profile to adopt with bending stress of workpiece material. This mold profile is redesigned by using the profile of workpiece after the deformed stage. An axisymmetric FEM model is established, and it consists of the new mold and workpiece. The uniform vacuum pressure is chosen as -95 kPa. The mold surface is redesigned with the conic constant $K = -3$ as displayed in **Figure 18**.

It can be noted that **Figure 19a** and **b** presents the deflection and deviation results between the workpiece and the new mold under supplied vacuum pressures, $P = -95$ kPa and $K = -3$.

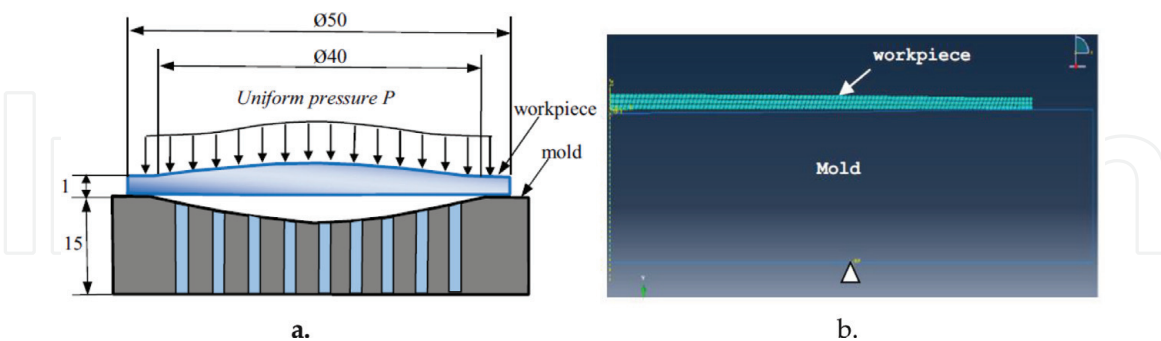


Figure 16.
(a) The simulation model and (b) FEM simulation model.

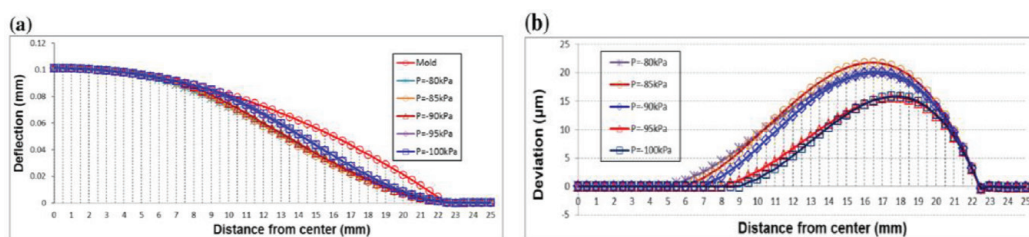


Figure 17.
(a and b) Deflection and deviation under different vacuum pressures ($K = -3$).

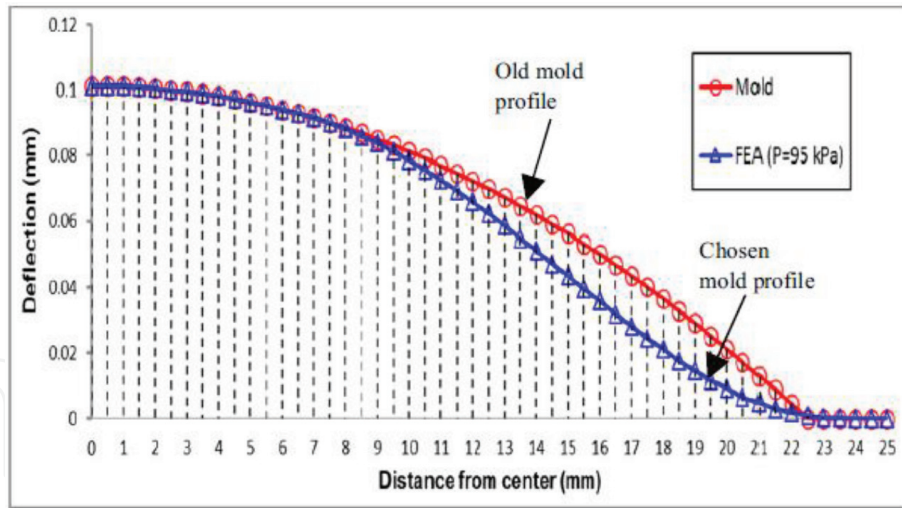


Figure 18.
 The modified mold is chosen.

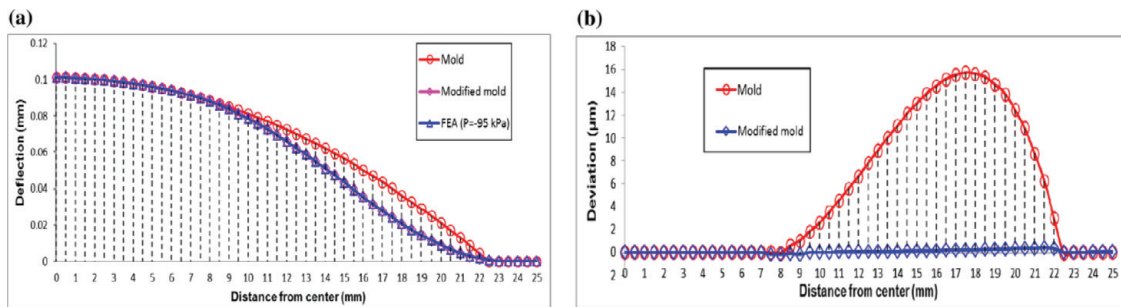


Figure 19.
 (a and b) Deflection and deviation results between the workpiece and modified mold.

The form accuracy of workpiece is enhanced by using the new mold surface. The maximum deviation is less than $P-V$ $0.35 \mu\text{m}$ while the former mold is about $15.02 \mu\text{m}$.

4.2 Experimental setup

Figure 20 presents that the experiment was conducted to a precision polishing machine Preci-Polish 300. The B270 glass with a diameter of 50 mm and a thickness

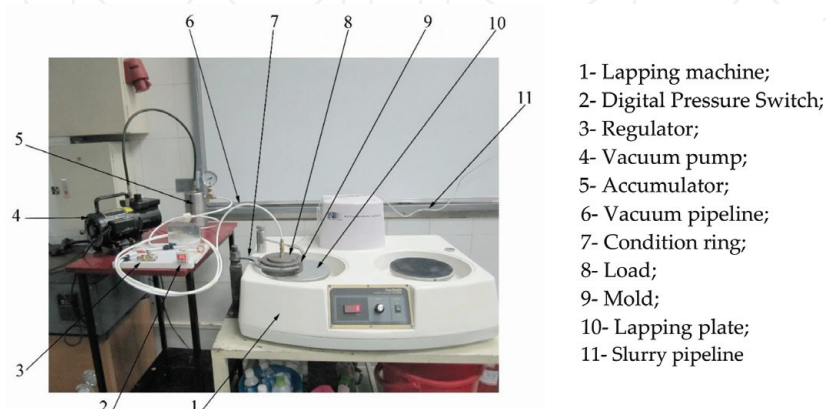


Figure 20.
 Experimental set-up in the lapping processes. 1-Lapping machine; 2-digital pressure switch; 3-regulator; 4-vacuum pump. 5-accumulator; 6-vacuum pipeline; 7-condition ring; 8-load; 9-mold; 10-lapping plate; and 11-slurry pipeline.

of 1.0 mm is utilized in the experiment process. In addition, **Table 4** points the parameters for the machining process, in which the vacuum pressure is fixed as -95 kPa.

According to the simulation results, the new mold surface with the conic constant $K = -3$ is chosen. The multi-small holes of the modified mold surface are fabricated to fix the workpiece during the machining process. The new mold is machined on a precision CNC machining center.

4.3 Experimental results

Figure 21a and **b** shows that experimental results are compared to FEA with new mold surface under applied vacuum pressure $P = -95$ kPa.

Based on the experimental and FEA results, the deviation of workpiece is less than P - V $0.01 \mu\text{m}$ within the radius of about 12 mm. The maximum deviation is P - V $0.6 \mu\text{m}$; however, the former mold is about $18.93 \mu\text{m}$. It is clear to see that the experimental results agree greatly with FEA results. Therefore, the form accuracy of the workpiece is significantly improved when the new mold profile is redesigned according to the FEA results with $P = -95$ kPa and $K = -3$.

Items	Lapping	Polishing
Abrasive	#1000 SiC	#10,000 CeO ₂
Abrasive concentration in slurry (wt%)	10%	10%
Machining load (N)	30	20
Rotating speed of lapping plate (rpm)	60	40
Machining time (min)	120	30

Table 4.
Lapping and polishing parameters.

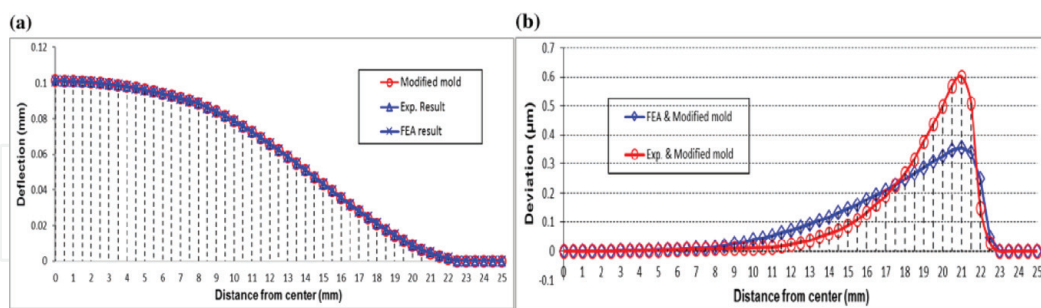


Figure 21.
(a and b) Experimental and FEA results with modified mold surface.

5. Conclusions

Based on the elasticity of the material, the elastic deformation machining is a method in which the vacuum pressure is used for fabricating complex aspheric surfaces. The amount of deflection of circular plate can be determined by solving the differential equations of an appropriate plate theory. The workpiece will be deformed into aspheric shape prior to the lapping process under the vacuum pressure. While the vacuum pressure is remained, the opposite side is polished to optical

flatness by the lapping wheel. Then, the vacuum pressure is not supplied and hence, the bottom surface will be formed into the aspheric shape and the top surface will be restored to its flat surface form. Therefore, the method is suitable for manufacturing of optical lens with large aperture and low thickness glass materials.

In the elastic deformation machining process without mold, the manufactured workpiece accuracy can be increased by adjusting the vacuum pressure during the machining process because of the changed workpiece thickness. The vacuum pressure is defined through FEA results. According to the FEA, the deformation curve of the workpiece is reached to the desired curve when the vacuum pressure is fixed at 42 kPa. Depending on reducing the vacuum pressure from 50 to 42 kPa and keeping stable through the entire machining process, the experimental results agree greatly with theoretical calculations. The best peak-valley value P - V 1.6 μm was achieved in this method.

In order to achieve form accuracy of the workpiece in the elastic deformation machining process with mold, the mold with its surface approximates the desired surface form of the lens which is used for improving the machining precision. The accuracy one can be innovated by modifying the mold profile to adopt with bending stress of workpiece material. This mold profile is redesigned by using the profile of workpiece after the deformed stage. According to the simulation results, the new mold surface with the conic constant $K = -3$ and vacuum pressure $P = -95$ kPa are used for the experimental process. In this case, the deviation of workpiece is less than P - V 0.01 μm within the radius of about 12 mm. The maximum deviation is P - V 0.6 μm ; however, the former mold is about 18.93 μm . It is clear to see that the experimental results agree greatly with FEA results.

IntechOpen

Author details

Duc-Nam Nguyen
Faculty of Mechanical Engineering, Industrial University of Ho Chi Minh City,
Vietnam

*Address all correspondence to: nguyennams@gmail.com

IntechOpen

© 2018 The Author(s). Licensee IntechOpen. This chapter is distributed under the terms of the Creative Commons Attribution License (<http://creativecommons.org/licenses/by/3.0>), which permits unrestricted use, distribution, and reproduction in any medium, provided the original work is properly cited. 

References

- [1] Aono Y, Negishi M, Takano J. Development of large-aperture aspherical lens with glass molding. *Advanced Optical Manufacturing and Testing Technology*. 2000;**4231**:16-23. DOI: 10.1117/12.402759
- [2] Suzuki H, Highuchi O, Huriuchi H, Shibutani H. Precision cutting of micro-axis-symmetric spherical surface with 3-axes controlled diamond tool. In: *Proceedings of the Second Euspen International Conference on European Society for Precision Engineering and Nanotechnology*; 27-31 May 2001; Italy. pp. 844-847
- [3] Anurag J. Experimental study and numerical analysis of compression molding process for manufacturing precision aspherical glass lenses [thesis]. Columbus: Ohio State University; 2006
- [4] Takashi M, Takenori O. Cutting process of glass with inclined ball end mill. *Journal of Materials Processing Technology*. 2008;**200**:356-363. DOI: 10.1016/j.jmatprotec.2007.08.067
- [5] Suzuki H, Moriwaki T, Yamamoto Y, Goto Y. Precision cutting of aspherical ceramic molds with micro PCD milling tool. *Annals of the CIRP*. 2007;**56**: 131-134. DOI: 10.1016/j.cirp.2007.05.033
- [6] Kim HS, Kim EJ, Song BS. Diamond turning of large off-axis aspheric mirrors using a fast tool servo with on machine measurement. *Journal of Materials Processing Technology*. 2004; **146**:349-355. DOI: 10.1016/j.jmatprotec.2003.11.028
- [7] Li L, Yi AY, Huang C, Grewell DA, Benatar A, Chen Y. Fabrication of diffractive optics by use of slow tool servo diamond turning process. *Optical Engineering*. 2006;**45**:113401. DOI: 10.1117/1.2387142
- [8] Bifano TG, Dow TA, Scattergood RO. Ductile-regime grinding: A new technology for machining brittle materials. *Journal of Engineering for Industry. Transactions of the ASME*. 1991;**113**:184-189. DOI: 10.1016/0141-6359(92)90161-0
- [9] Lambropoulos JC, Fang T, Funkenbusch PD, Jacobs SD, Cumbo MJ, Golini D. Surface micro-roughness of optical glasses under deterministic micro-grinding. *Applied Optics*. 1996; **35**:4448-4462. DOI: 10.1364/AO.35.004448
- [10] Namba Y, Abe M, Kobayashi A. Ultra-precision grinding of optical glasses to produce super-smooth surfaces. *Annals of the CIRP*. 1993;**42**: 417-420. DOI: 10.1016/S0007-8506(07)62475-5
- [11] Chen WK, Kuriyagawa T, Huang H, Yoshihara N. Machining of micro aspherical mould inserts. *Journal of Precision Engineering*. 2005;**29**:315-323. DOI: 10.1016/j.precisioneng.2004.11.002
- [12] Brinksmeier E, Mutlugunes Y, Klocke F. Ultra-precision grinding. *CIRP Annals-Manufacturing Technology*. 2010;**59**:652-671. DOI: 10.1016/j.cirp.2010.05.001
- [13] Bingham R, Walker D, Kim D. Novel automated process for aspheric surfaces. In: *Proceedings of SPIE – The International Society for Optical Engineering*. 2000;**4093**:445-448. DOI: 10.1117/12.405237
- [14] Walker D, Brooks D, King A. The “Precessions” tooling for polishing and figuring flat, spherical and aspheric surfaces. *Optics Express*. 2003;**11**: 958-964:958-964. DOI: 1364/OE.11.000958
- [15] Nelson J, Scordato M, Schwertz K. Precision lens molding of asphero

diffractive surfaces in chalcogenide materials. *Optifab*. 2015;96331L. DOI: 10.1117/12.2195764

[16] Mahajan P, Dora PT, Sandeep TS. Optimized design of optical surface of the mold in precision glass molding using the deviation approach. *International Journal for Computational Methods in Engineering Science and Mechanics*. 2015;16:53-64. DOI: 10.1080/15502287.2014.976677

[17] Yi AY, Tao B, Klocke F. Residual stresses in glass after molding and its influence on optical properties. *Procedia Engineering*. 2011;19:402-406. DOI: 10.1016/j.proeng.2011.11.132

[18] Kunz A. Aspheric freedoms of glass-precision glass moulding allows cost-effective fabrication of glass aspheres. *Optik & Photonik*. 2009;4:46-48. DOI: 10.1002/opph.201190063

[19] Mori Y, Yamamura K, Endo K, Yamauchi K, Yasutake K, Goto H, Kakiuchi H, Sano Y, Mimura H. Creation of perfect surfaces. *Journal of Crystal Growth*. 2005;275:39-50. DOI: 10.1016/j.jcrysgro.2004.10.097

[20] Ventsel E, Krauthammer T, editors. *Thin Plates and Shells: Theory, Analysis, and Applications*. 1st ed. Boca Raton: CRC Press; 2001. p. 688

[21] Nguyen DN, Lv BH, Yuan JL, Wu Z, Lu HZ. Experimental study on elastic deformation machining process for aspheric surface glass. *International Journal of Advanced Manufacturing Technology*. 2013;65:525-531. DOI: 10.1007/s00170-012-4191-3

[22] Schott. Schott B270 Super-white Properties [Internet]. 2015. Available from: <https://psec.uchicago.edu/glass/SchottB270Properties-KnightOptical.pdf> [Accessed: 24-05-2018]

[23] Nguyen DN. Study on improving the precision of form surface produced

in elastic deformation molding process. *International Journal of Advanced Manufacturing Technology*. 2017;93:3473-3484. DOI: 10.1007/s00170-017-0766-3

[24] Kweon G, Kim CH. Aspherical lens design by using a numerical analysis. *Journal of the Korean Physical Society*. 2007;51:93-103. DOI: 10.3938/jkps.51.93